BIOCHEMISTRY
including biophysical chemistry & molecular biology

Article

pubs.acs.org/biochemistry

Solvent-Induced α- to 3_{10}-Helix Transition of an Amphiphilic Peptide

Ricky B. Nellas,[†,‡] Quentin R. Johnson,[‡,§] and Tongye Shen*[,†,‡]

[†]Department of Biochemistry and Cellular and Molecular Biology, The University of Tennessee, Knoxville, Tennessee 37996, United States

[‡]The University of Tennessee-Oak Ridge National Laboratory Center for Molecular Biophysics, Oak Ridge National Laboratory, Oak Ridge, Tennessee 37830, United States

[§]The University of Tennessee-Oak Ridge National Laboratory Graduate School of Genome Science and Technology, The University of Tennessee, Knoxville, Tennessee 37996, United States

Supporting Information

ABSTRACT: The amphiphilic peptide of the triacylglycerol lipase derived from *Pseudomonas aeruginosa* plays a critical role in guarding the gate for ligand access. Conformations of this peptide at several water−oil interfaces and in protein environments were compared using atomistic simulations with explicit solvents. In oil-containing solvents, this peptide is able to retain a folded structure. Interestingly, when the peptide is immersed in a low-polarity solvent environment, it exhibits a "coalesced" helix structure, which has both α- and 3_{10}-helix components. The observation that the 3_{10}-helical conformation is populated in a highly nonpolar environment is consistent with a previous report on polymethylalanine. Frequent interconversions of the secondary structure (between α-helix and 3_{10}-helix) of the peptide are also observed. We further studied how this solvent-induced structural transition may be connected to the trigger mechanism of lipase gating and how the lipase senses the hydrophobic−hydrophilic interface.

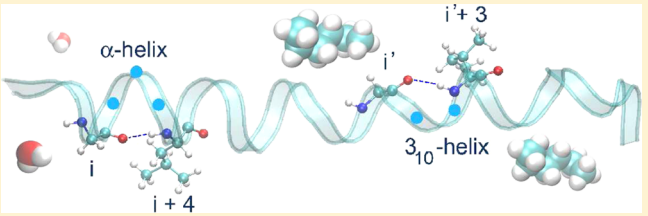

Amphiphilic (also known as amphipathic) peptides are surprisingly abundant in nature's design of biomolecules.[1,2] Although hidden from the plain view of sequence information, a distinct helix containing a hydrophilic face and a hydrophobic face is revealed when the peptide is properly folded.[1,3−5] Because of this unique amphiphilic pattern, these peptides can act as a barrier between polar and nonpolar components of a protein and can also have unique roles for proteins that function at interfaces.[1] In fact, several important peptides, from hormones to cytolytic toxins to neurotransmitters, are amphiphiles.[1,6,7] Also, many of the amphiphilic helices are the critical components of proteins,[1] from lung surfactant protein (water−air interface)[8,9] to channel proteins (multihelix packing)[10,11] to antifreeze proteins (ice structuring).[12,13]

Canonical helices such as 3_{10}-, α-, and π-helices are stabilized by backbone hydrogen bonding between the carbonyl group (C═O) of residue i and the amine group (N−H) of downstream residues i + 3, i + 4, and i + 5, respectively.[14,15] A typical α-helix has 3.6 residues per turn (100° rotation per residue) and a 5.4 Å pitch (1.5 Å per residue). The sequence information of an α-helix can be displayed in an extended wheel diagram, as shown in Figure 1a. Each complete layer of the wheel has 18 residues. The N-terminus belongs to the innermost layer. In contrast, a 3_{10}-helix has three residues per turn (120° rotation per residue) and a longer pitch of 5.8−6 Å (2 Å per residue).[16] Thus, a 3_{10}-helix displayed in an extended wheel diagram has three residues per layer. Other noncanonical helix structures have also been suggested, such as the 11-mer repeat α11/3-helix.[17,18]

Because the H-bonding of an α-helix needs five residues for initiation, extremely short segments are more likely to be found in the 3_{10}-helical conformation while longer helical structures are assumed to be predominantly α-helical.[19] Of the peptides that are known to adopt a helical conformation, 10% are 3_{10}-helical.[20,21] A pioneering study of the interconversion between the α- and 3_{10}-helix using a capped decamer of α-methylalanine (a nonproteinogenic amino acid) examined the thermodynamics of these two conformations in vacuum and in explicit solvents such as water, acetonitrile, and dichloromethane.[22] In the crystal structures of artificial peptides that contain nonproteinogenic amino acids α-monoalkyl and α,α-dialkyl, both α- and 3_{10}-helices are commonly observed.[22] In a crystallographic examination, a section of the apo form of lactate dehydrogenase exhibits an α-helical conformation.[23] Upon binding to lactate and nicotinamide adenine dinucleotide (NAD), it forms a "coalesced" helix: a part of it becomes a 3_{10}-helix, and the rest remains α-helical.[23] Also, the emergence of a molten helix has been observed in the open to closed transformation of aspartate aminotransferase.[24]

The general preference of α- versus 3_{10}-helix as well as the dynamics of the transition between these two states are still not

Received: April 29, 2013
Revised: August 13, 2013
Published: September 25, 2013

   dx.doi.org/10.1021/bi400537z | *Biochemistry* 2013, 52, 7137−7144

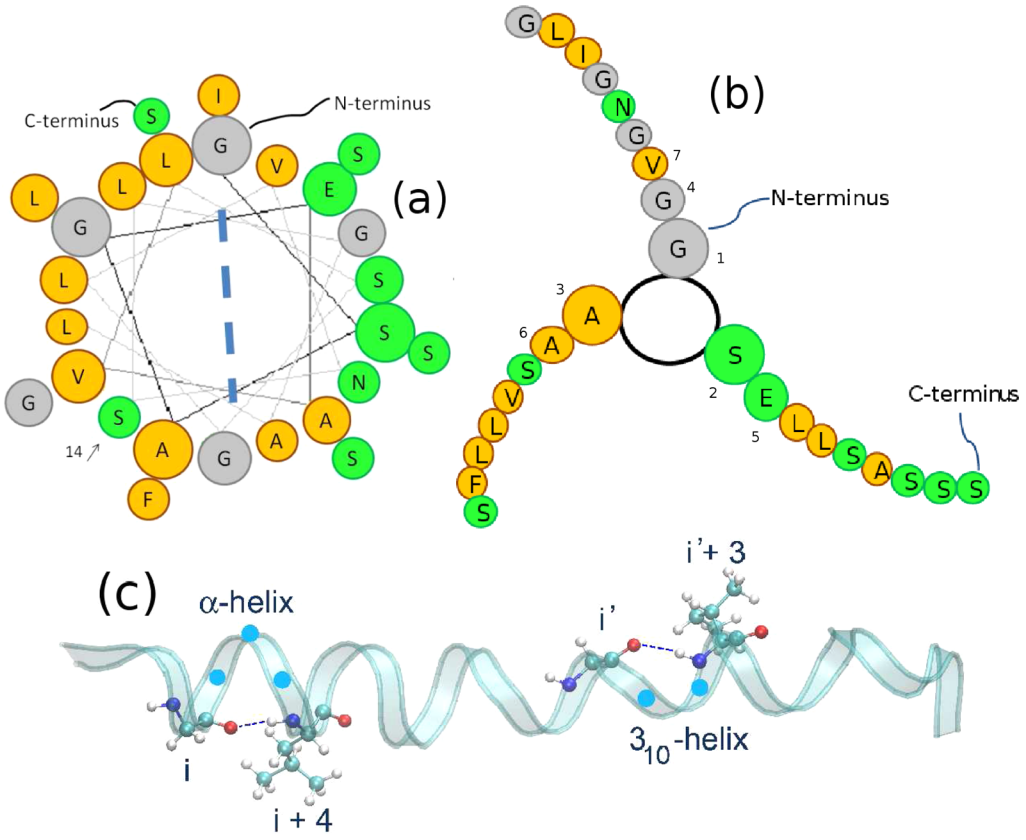

Figure 1. (a) α-Helical and (b) 3_{10}-helical wheel representations of the 26-residue peptide from *Pseudomonas aeruginosa* lipase. For the α-helical wheel, each layer of the wheel has 18 residues. For the 3_{10}-helical wheel, each layer has three residues with the first few residues labeled. This visualization shows that this naturally occurring peptide has an amphiphilic character, wherein the hydrophilic residues (green) are on one side of the wheel and the hydrophobic residues (orange) are on the other side of the wheel. (c) Representative snapshot of the 26-residue peptide exhibiting both α-helical (i–i + 4) and 3_{10}-helical (i–i + 3) conformations. Circles in the ribbon represent Cα atoms.

well understood, especially in the context of a naturally occurring amphiphilic helix. Crystallographic data suggest that peptide length and capping residues influence the resulting conformation of the helix in general.[25−28] Overall, longer peptides can manifest a mixture of α- and 3_{10}-helical conformations, while short peptides may favor the 3_{10}-helix.[29] There is a critical length of the peptide indicating the shift of the preference. On the basis of extensive oligo-α-methylalanine studies, the critical length at which α- and 3_{10}-helical conformers have nearly equal potential energy can be computed. The results are slightly dependent on force field, which give critical lengths of 12, 8, and <7 amino acids for the parameters of AMBER all-atom,[30] AMBER united-atom,[31] and OPLS force fields,[32] respectively.

Previous experimental[16,33,34] and computational[22] studies demonstrated that the polarity of the solvent can affect the preferred conformation, α- or 3_{10}-helix. For poly-α-methylalanine, changing the solvent from dichloromethane to water increases the chance to form α-helix over 3_{10}-helix.[22] In addition, decamethylalanine in water or deuterated dimethyl sulfoxide favors α-helix over 3_{10}-helix, while in a nonpolar environment such as dichloromethane or deuterated chloroform, the 3_{10}-helical conformation is more stable.[35] There is a consensus that, for these simple artificial peptides, α-helix dominates in a polar environment while 3_{10}-helix can be more populated in anhydrous solvents.[22,26,27,33,35] Still, few studies of how complex solvent environments (including low-polarity solvents and interfaces) affect the conformations of a natural peptide that is amphiphilic in nature have been reported.

SYSTEMS AND METHOD

In this study, atomistic simulations were performed on amphiphilic peptides from *Pseudomonas aeruginosa* lipase PAO1 and from human apolipoprotein in various explicit solvents and interfacial systems. The initial conformation of the 26-residue peptide was obtained from a lipase PAO1 [Protein Data Bank (PDB) entry 1EX9, residues 124−149, GSAGE AVLSG LVNSL GALIS FLSSG S].[36] We also examined a 26-residue peptide from a human apolipoprotein (PDB entry 1AV1, residues 90−115, LEEVK AKVQP YLDDF QKKWQ EEMEL Y)[37] for comparison. The AMBER 99sb force field was used for the peptide.[38] The TIP3P model[39] was used for the parameter of water, while hexane and benzene were parametrized using the antechamber module of AMBER 10.[40] A sodium ion was added to neutralize each α5 system.

Various systems were created by solvating the 26-residue α5 peptide of PAO1 (hereafter termed "A") in water (A100W), in a minute amount of hexane in water (A5H), at a planar hexane−water interface (A50H), in a minute amount of water in hexane (A95H), and in hexane (A100H). The initial solvation procedure using multiple solvents is similar to that of ref 41. A complete list of the systems investigated is shown in Table S1 of the Supporting Information. Representative snapshots of the initial and evolved configurations of interfacial systems (A5H, A50H, and A95H) are shown in Figure S1 of

dx.doi.org/10.1021/bi400537z | *Biochemistry* 2013, 52, 7137−7144

the Supporting Information. The setups for the 26-residue peptide from the human apolipoprotein in water (L100W) and in hexane (L100H) were performed in a manner similar to that of peptide α5.

Minimization, heating, *NPT* (p = 1 bar) equilibration, and production runs were performed using the sander module of AMBER 10.[40] All simulation production runs were performed at 300 K and a constant volume (*NVT* ensemble). The temperature was regulated using the Langevin thermostat. The long-range interactions were treated using the particle mesh Ewald method. A nonbonded cutoff of 8 Å and a time step of 2 fs are used. Frames are collected at 1 ps intervals. Data collected from the 50 ns equilibration run were discarded, and statistical analyses were performed on the last 150 ns of the simulations.

Additionally, data about the conformations of the peptide section from the previous simulation of the whole 285-residue enzyme[41] (hereafter termed "E") will be used for comparison. As an example, the notation "E100H" refers to the system of the enzyme (E) placed in pure hexane (100H).

RESULTS AND DISCUSSION

We will discuss below how complex solvent interfaces perturbed the structural integrity of peptide α5 of *P. aeruginosa* lipase. To the best of our knowledge, this is a first report of the solvent-induced conformational switch of a functional and naturally occurring amphiphilic peptide.

A Coalesced Helical Structure. We first report the coexistence of the α- and 3_{10}-helical conformers in peptide α5. As shown in Figure 1a (the helical wheel representation[4]), this 26-residue peptide has an amphiphilic characteristic when it is folded as an α-helix. The corresponding 3_{10}-helical arrangement is depicted in Figure 1b. One of the three branches is mainly hydrophobic. Another one is mainly hydrophilic, while the third branch contains all the glycine residues. One can also show the amphiphilicity in the noncanonical 11-mer repeat helix.[17]

To quantify the secondary structure of this helical peptide, we monitored the formation of backbone H-bonds, as illustrated in Figure 1c. Here, two approaches were used to determine whether an H-bond is formed for a particular configuration. Using a set of geometric criteria, an H-bond is formed when the distance ($r_{O\cdots H}$) between the carbonyl oxygen of residue i and the amide hydrogen of residue i + 4 (or i + 3) is ≤3.5 Å, and the angle ($\theta_{N-H\cdots O}$) is between 120° and 180°. An alternative (energetic) criterion implemented in the DSSP algorithm[42] deems an H-bond formed when energy E between the C═O group of residue i and the N−H group of i + 4 or i + 3 is lower than −0.5 kcal/mol. Here E is $27.888 \times (1/r_{ON} + 1/r_{CH} - 1/r_{OH} - 1/r_{CN})$ kcal Å mol^{-1}. H-Bond formation is calculated every picosecond, and the mean value over the 150 ns of data is reported here. Some of the hydrogen bonds are clearly bifurcated[15,43] (the C═O group of residue i simultaneously forms H-bonds with the N−H groups of both i + 3 and i + 4).

As shown in panels a and c of Figure 2, the percentage of α-helical backbone H-bonds in hexane (A100H) decreases gradually from the N- to C-terminus, but unfolding was not observed from visual inspection. To resolve the apparent conflicting information between the loss of backbone i−i + 4 H-bonding and structural integrity, we examined possible i−i + 3 backbone H-bonds. As shown in panels b and d of Figure 2, the propensity of 3_{10}-helix indeed increases from the N- to C-terminus. Although it seems that the energetic criterion is more stringent than the geometric criterion, both give a consistent

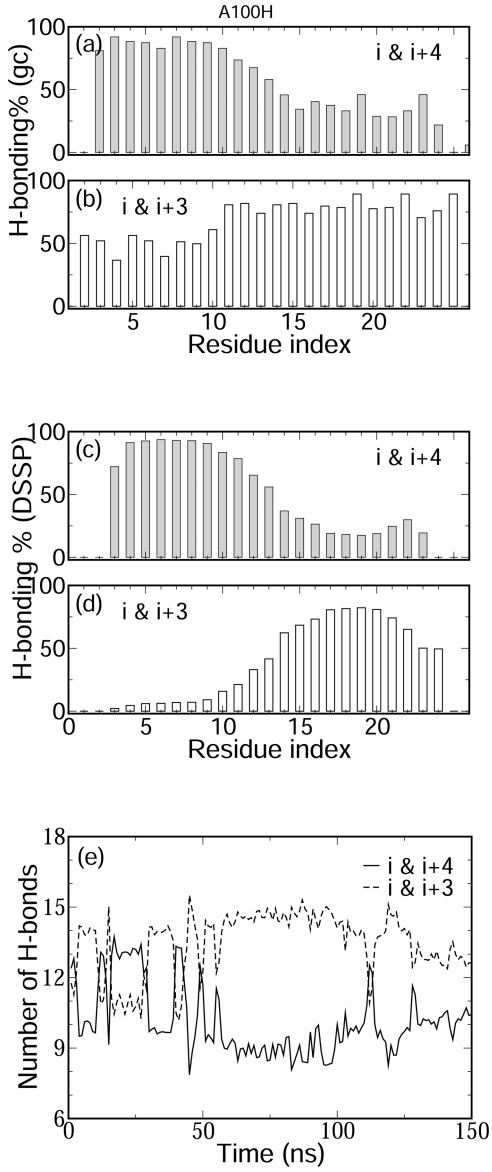

Figure 2. Percentages of backbone H-bonds formed between residues i (CO) and i + 4 (NH) of the α-helical conformation and i (CO) and i + 3 (NH) of the 3_{10}-helical conformation in A100H. (a and b) For the geometric criterion, an H-bond is formed when the distance ($r_{O\cdots H}$) between the carbonyl oxygen of residue i and the amide hydrogen of residue i + 4 (or i + 3) is ≤3.5 Å, and the carbonyl oxygen of residue i and the amide NH group of residue i + 4 (or i + 3) forms an angle ($\theta_{N-H\cdots O}$) of around 120−180°. (c and d) H-Bonding using the DSSP energetic criterion. H-Bond formation is calculated every picosecond and averaged over 150 ns of simulation data. (e) Time evolution of the total number of H-bonds formed (α- and 3_{10}-helical conformations) in the peptide for A100H. H-Bond formation is calculated every picosecond, and the mean value from a nanosecond window is presented here.

trend. Most of our results were reported from the geometric criterion, but the use of the energetic criterion does not change the findings.

We further studied the dynamics of backbone H-bond formation. H-Bonding using the geometric criterion was calculated, and the mean value from a running nanosecond window is presented here. The time evolution of the H-bond (shown in Figure 2e) demonstrates that the peptide contains both α- and 3_{10}-helical conformations. While the total number

dx.doi.org/10.1021/bi400537z | *Biochemistry* 2013, 52, 7137−7144

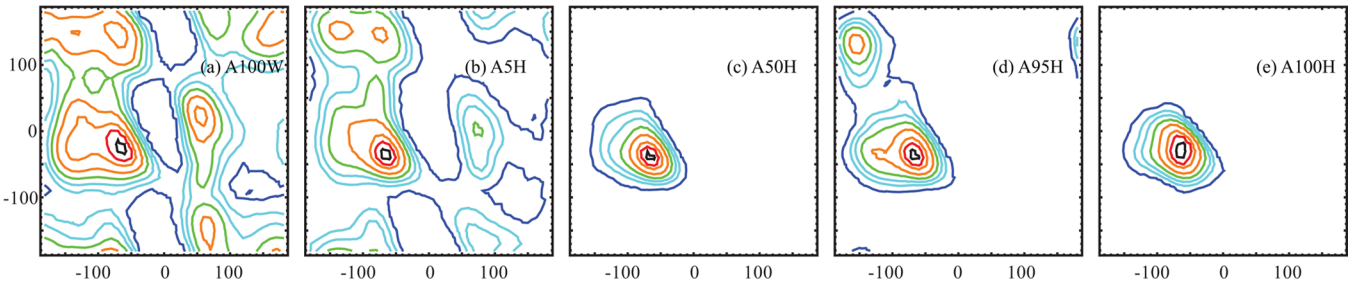

Figure 3. Free energy profiles of Ramachandran space for (a) A100W, (b) A5H, (c) A50H, (d) A95H, and (e) A100H at 300 K. The Ramachandran plots of all the residues of the peptide (except the ones at the termini) were used to construct each profile. The contour lines are 0.1 (black), 0.5 (red), 1.0 and 2.0 (orange), 3.0 (green), 4.0 and 5.0 (cyan), and 6.8 (blue) kcal/mol above the corresponding global minimum.

of backbone H-bonds is conserved approximately, there is a switch between the dominant type of H-bonds on the order of tens of nanoseconds. Because the secondary structural elements of the peptides interconvert between α- and 3_{10}-helical conformations, we further examined this switch at a more site-resolved resolution. We performed a similar analysis of the dynamics of backbone H-bond formation by obtaining separate statistics for the N- and C-terminal halves of the peptide (Figure S2 of the Supporting Information). Interestingly, when the N-terminal half is largely α-helical, the C-terminal half is 3_{10}-helical and vice versa. On average, the N-terminus is rich in α-helical conformers while the C-terminus is mostly 3_{10}-helical. The existence of this dynamic switch at the level of secondary structure can be corroborated by the dynamics of the root-mean-square deviations (rmsds) from the initial α-helical structure (Figure S3 of the Supporting Information). The dynamic fluctuation of the rmsd strongly correlates with the dynamics of hydrogen bonding. As a supplement to the dynamic H-bonding analysis, it seems that the rmsd values of <4 Å pertain to the α-helix-rich structure while values of >4 Å suggest a conformation rich in 3_{10}-helical secondary structures.

Besides hydrogen bonding and rmsd, the Ramachandran plot (backbone torsional angles ϕ and ψ) is often used to characterize secondary structure. The coalesced helical structure of A100H is also evident from the Ramachandran plots shown in Figure 3. Though both are at helical regions, the locations of the free energy minima in A50H ($-65°$, $-40°$) and A100H ($-60°$, $-25°$) are dramatically different. An important $\phi-\psi$ signature that distinguishes different helical structures is the value of $\phi + \psi$. The population of typical α-helical structures peaks around $\phi + \psi = -104°$, while 3_{10}-helix gives a value of $-75°$.[44] Here, A50H gives $\phi + \psi = -105°$, which is consistent with the typical value of the α-helix, while A100H gives a value of $-85°$, which is between the limits of α and 3_{10}-helices. Thus, the population for the A100H system is shifted to the top right, which signals an enhanced sampling of the 3_{10}-helical conformation. Using these complementary analyses, our result clearly shows a "coalesced" helix with subregions of different types of helices that interconvert.

Conformations of Amphiphilic Peptides in Complex Solvent Milieus. Besides the study of the conformations of α5 in hexane, which is reported in the previous subsection, we also studied α5 at different hydrophobic–hydrophilic interfaces. When the α5 peptide is in a significantly nonpolar environment (A100H, A95H, or A50H), α5 has an α-helical structure, as shown in Figure 4a–c (using the geometric criterion) and Figure 3. Meanwhile, the end-to-end distance (the distance between the backbone nitrogen on both ends, 1N–26N) shows little fluctuation. As shown in Figure 5, the mean end-to-end

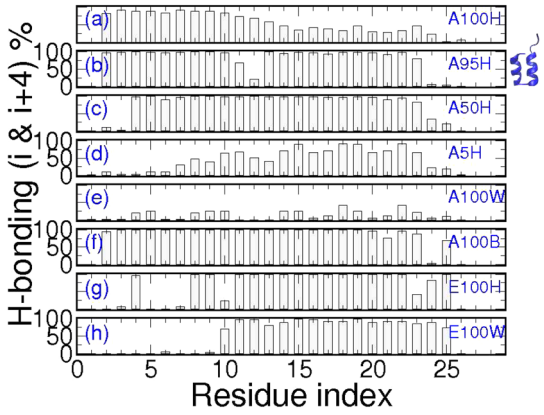

Figure 4. Percentage of backbone H-bonds made between residues i (CO) and $i + 4$ (NH) constituting the α-helical conformation in various solvent milieus. In all systems, H-bond formation (geometric criterion) is calculated every picosecond. Mean values are obtained from 50 ns of data in E100H and E100W (previous study[41]) and 150 ns of data in other systems.

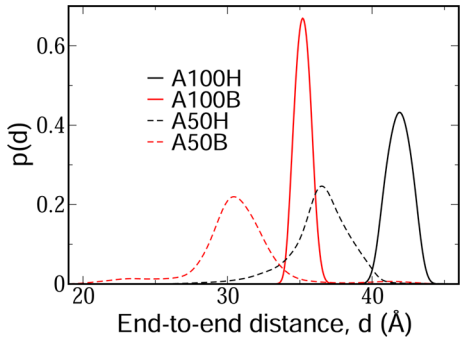

Figure 5. Distribution of the end-to-end distances between the backbone nitrogen on both ends (1N–26N) of 26-residue peptide α5 under different solvent conditions.

distance is ~42 Å for A100H and ~37 Å for A50H. A much shorter mean end-to-end distance of A95H (~8 Å) is caused by a predominant helix–turn–helix conformation. As indicated in Figure 4b, there is a break in the helix around the midsection. By visual inspection, it was observed that water molecules clamp the middle of the peptide, around position 14 (Ser137), which is a hydrophilic residue located at the center of the hydrophobic face.

On the other hand, when the α5 peptide is in a significantly polar environment (A5H and A100W), it is a disordered peptide with a diverse set of ϕ and ψ values (Figure 3). Under this polar condition, most of its residues do not participate in

dx.doi.org/10.1021/bi400537z | Biochemistry 2013, 52, 7137–7144

backbone H-bonding (Figure 4d,e), and its structure is highly perturbed with a broad end-to-end distance distribution spanning ∼5−40 Å. This shows that the presence of water molecules plays an important role in the conformational exploration of peptides.[45,46] The α-helix disruption in this system can be attributed to the presence of a stronger intermolecular (peptide−water) rather than intramolecular (intrapeptide) interaction.

So far, we have found that the amphiphilic peptide, α5 of lipase PAO1, is stable in pure hexane and at a planar hexane−water interface but not in pure water. It is important to see how general this conclusion is. Besides peptide α5 of PAO1, we also studied peptide α5 of an extremophilic strain of *P. aeruginosa* (PAL-LST03),[47,48] Am100H, which has only one different residue, V130I. Not surprisingly, the change from valine to isoleucine did not change the nature of the helical conformation reported so far. However, not all amphiphilic helices share the stability of α5 in anhydrous solvents. Our results for L100H indicate that, unlike α5, the selected peptide from the human apolipoprotein mostly unfolds in pure hexane. However, sections of the peptide, residues 3−6 (α-helix) and 13−20 (3_{10}-helix), still display a strong secondary structure, while all the amphiphilic peptides examined in this study are stable at a planar water−oil interface. Generally, the amphiphilic peptides examined here are unfolded in water. Interestingly, residues 3−6 and 9−12 of the human apolipoprotein participate in α-helix formation, while residues 16−19 are 3_{10}-helical in water. This indicates that the peptide composition and sequence (side chain identity) may be crucial. Also, it seems that the presence of both α-helical and 3_{10}-helical conformations is ubiquitous in proteinogenic amphiphilic peptides. Note that the examined section of the apolipoprotein has a higher percentage of hydrophilic residues than that of α5.

Interfacial Water. To understand the role of interfacial water on the conformations of the peptide, we applied a solvent mapping procedure to locate the peptide hydration sites, a region around the peptide where water molecules preferentially reside.[49] For the systems that remain α-helical, we can further express the density of water in terms of cylindrical coordinates (d, ϕ, z) using an ideal α-helical reference state (created by the LEAP program), where d is the radial coordinate, ϕ is the azimuth, and h is the height. We set the coordinates by aligning the direction of the ideal helix as the cylindrical axis $\hat{\mathbf{z}}$ and set the Cα atom of the first residue, Gly, at the direction of azimuth $\phi = 0$. After the integration along z, we obtain the water density $\rho(\phi,d)$. We applied this analysis to the A50H system. This integration procedure is appropriate only if the peptide is not dramatically different from that of the ideal helix reference. Generally, we can always express the water density in three-dimensional Cartesian coordinates.

Water densities surrounding peptide α5 in A5H, A50H, and A95H systems are shown in Figure 6. For A5H, the presence of water molecules in most regions of the peptide results in a lower backbone α-helical H-bond formation and an enhanced conformational exploration (Figure 3b) of the peptide as compared to that of A50H. For A95H, only the termini and midsection of the peptide are highly hydrated, which leads to broken midbackbone and terminal backbone H-bonds and thus favors a helix−turn−helix conformation. This preferential hydration in A95H gives rise to a reduction of the conformational exploration of the peptide (Figure 3b) and the retention of many of its backbone H-bonds (Figure 4b).

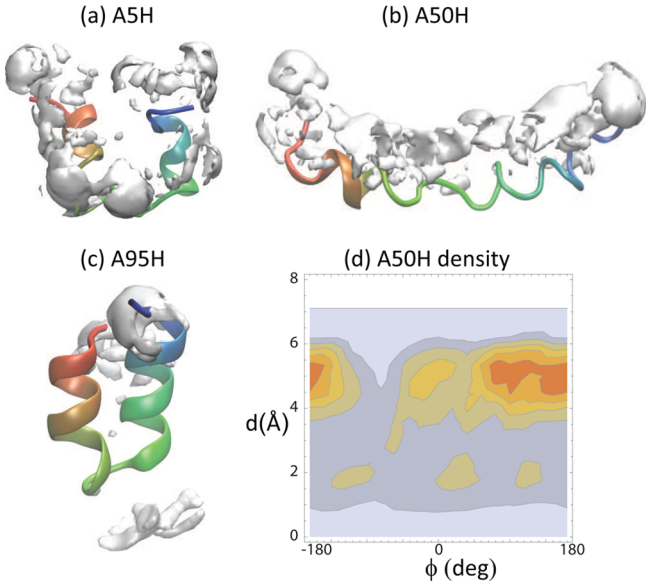

Figure 6. Water densities surrounding peptide α5 in the A5H, A50H, and A95H systems (a−c, respectively) displayed as iso-density contours. For each system, the structure of the peptide at the end of a 200 ns simulation was used as the reference state in calculating the water density around the peptide. (d) Density of water molecules of A50H expressed in the cylindrical coordinates, $\rho(\phi,d)$. The color orange indicates a high density of water.

For A50H, the α-helical peptide stays at an almost planar interface. As shown by $\rho(\phi,d)$ in Figure 6d, the region ($-160° < \phi < 60°$) has a low water density. This is the region where the hydrophobic residues are located, as shown in the wheel diagram (Figure 1a). This solvent structure in the A50H system thus stabilizes this amphiphilic peptide, which has limited conformational exploration (Figure 3c) and a high level of α-helical H-bonding (Figure 4c).

Solvent Specificity. Previous evidence shows the activity preference in the pairing of specific lipases and organic solvent types (aromatic vs aliphatic).[50,51] For example, the activity of PAL-LST03[50] monotonously increases with the methyl:phenyl ratio (from benzene to toluene to *p*-xylene), while *Acinetobacter baylyi*[51] shows the opposite trend. Motivated by these reports, we also examined the specificity of the anhydrous solvents on the conformations of peptide α5. By monitoring the percentage of backbone H-bonds (α and 3_{10} type) of peptide α5 in hexane (A100H) and benzene (A100B), we compared the helical propensity in aliphatic and aromatic solvents. While the peptide in hexane exhibits both α- and 3_{10}-helical conformations, the peptide in benzene is mostly α-helical, as indicated by H-bonding (Figure 4f). The end-to-end distance results also confirmed that the peptide in hexane is more elongated than when it is in benzene, with mean distances of ∼42 and 35 Å (Figure 5), respectively. Additional studies of peptide α5 at water−hexane (A50H) and water−benzene (A50B) interfaces showed both are rich in α-helical conformers. The terminal H-bonds are broken in A50H and remain intact in A50B (Figure 4c).

Here we did not observe the transition from the initial α-helical conformation to a 3_{10}-helix-rich conformation for A100B; rather, α-helix shows strong stability. It is possible that there is a kinetic factor that makes benzene a strong immobilizing medium. The viscosity of benzene (0.59 cP) is higher than that of hexane (0.29 cP).[52] The potential transition

dx.doi.org/10.1021/bi400537z | *Biochemistry* 2013, 52, 7137−7144

from the initial α-helix to 3_{10}-helix-rich structure may still occur, but in a longer time than the submicrosecond time scale reported here. The absence of 3_{10}-helix in benzene may also have an equilibrium factor: the larger relative polarity of benzene (0.111) compared to that of hexane (0.009).[53] At the atomistic level, carbon and hydrogen atoms of benzene have larger absolute partial charges than their hexane counterparts.

Enzyme environment. Finally, we report the structure of the α5 section of the lipase from the previous whole protein simulations (100 ns).[41] As shown in Figure 4, regardless of solvent conditions, the backbone H-bonds tend to be more stable when the peptide is a part of the enzyme than the stand-alone peptide. A localization of the ends and a decrease of solvent exposure due to the presence of the rest of the lipase may contribute to the enhanced stability. The α5 section of the enzyme exhibits the coexistence of α- and 3_{10}-helix for all four solvent conditions. Here, the calculated mean number, N of *i*-*i* + 4 (*i*-*i* + 3) H-bond values are N(E100W) = 11.5 (5.3), N(E5H) = 12.8 (4.9), N(E95H) = 16.0 (6.0), and N(E100H) = 13.7 (6.4).

It is interesting to speculate the importance of the coexistence of α- and 3_{10}-helical structural elements to the function of the lipase gating. One possibility is that the transition from α- to 3_{10}-helix is the environmental sensing or trigger mechanism of gate opening. Another possibility is that the α-helix and 3_{10}-helix are stable and predominant under different solvent conditions and thus enhance the overall stability of the folded helical conformation. We performed further analysis to examine whether there is any simple correlation between the level of gate opening measured by gorge radius[41] and the conformation of α5 in four solvent environments: E100W, E5H, E95H, and E100H. The mean gorge radius values are as follows: r(E100W) = 0.7 Å, r(E5H) = 1.4 Å, r(E95H) = 2.3 Å, and r(E100H) = 1.3 Å. Thus, it seems that gate opening is promoted when the helix (either α- or 3_{10}-helix) is stable. Thus, a structural buffering mechanism to stabilize the helical structure might be essential to keep the gate open.

CONCLUSIONS

In summary, this work examines the solvent-induced conformational preference in a naturally occurring amphiphilic peptide from *P. aeruginosa* lipase. Here we have compared the behavior of the peptide from the perspectives of peptide chemical identity, solvent interface composition, solvent specificity, and enzyme environment. We found that the peptide can exhibit an interesting transition between α- and 3_{10}-helix-rich conformations, which is consistent with previous studies of the stabilizing effect of the 3_{10}-helical conformation by low-polarity solvents. At water−oil interfaces, the retention or disruption of H-bonds at a specific site is caused by the preferential distribution of water molecules around the peptide and, essentially, the specific interaction of the residues with water.

The peptide behaves differently when it is a part of the enzyme. Interestingly, the α5 section of the enzyme shows molten helix characteristics. We further discussed two possible scenarios (gating trigger mechanism vs conformational buffering) of how this partial 3_{10}-helix feature may be important for lipase function. We concluded that helical interconversion is a structural buffering act in a variety of solvent environments to keep the access channel open.

ASSOCIATED CONTENT

Supporting Information

Compositions of the systems studied (Table S1), representative simulation setup (Figure S1), time evolution of the total number of H-bonds formed (α- and 3_{10}-helical conformations) for the N-terminal half (residues 1−13) and the C-terminal half (residues 14−26) of the peptide in A100H (Figure S2), and time evolution of the rmsd (projected on the crystal structure) of the peptide in hexane (A100H) (Figure S3). This material is available free of charge via the Internet at http://pubs.acs.org.

AUTHOR INFORMATION

Corresponding Author

*E-mail: tshen@utk.edu. Phone: (865) 974-4088. Fax: (865) 974-6306.

Funding

Financial support from the Petroleum Research Fund administered by the American Chemical Society (52616-DNI6) is gratefully acknowledged. Q.R.J. is supported by National Science Foundation-funded graduate fellowship program SCALE-IT.

Notes

The authors declare no competing financial interest.

ACKNOWLEDGMENTS

We acknowledge the computational support provided by The University of Tennessee-Oak Ridge National Laboratory Center for Molecular Biophysics and by allocations of advanced computing resources (TG-MCB120011, TG-MCA08X032, UT-TENN0049) on Kraken at the National Institute for Computational Sciences.

ABBREVIATIONS

PAL, *P. aeruginosa* lipase; rmsd, root-mean-square deviation.

REFERENCES

(1) Epand, R. M. (1993) *The Amphiphatic Helix*, CRC Press, Inc., Boca Raton, FL.
(2) Richardson, J. S. (1985) Describing patterns of protein tertiary structure. *Methods Enzymol. 115*, 341−358.
(3) Eisenberg, D., Weiss, R. M., and Terwilliger, T. C. (1982) The helical hydrophobic moment: A measure of the amphiphilicity of a helix. *Nature 299*, 371−374.
(4) Shiffer, M., and Edmunson, A. B. (1967) Use of helical wheels to represent the structures of proteins and to identify segments with helical potential. *Biophys. J. 7*, 121−135.
(5) Dunnill, P. (1968) The use of helical net-diagrams to represent protein structures. *Biophys. J. 8*, 865−875.
(6) Kini, R. M., and Evans, H. J. (1989) A common cytolytic region in myotoxins, hemolysins, cardiotoxins and antibacterial peptides. *Int. J. Pept. Protein Res. 34*, 277−286.
(7) Bernheimer, A. W., and Rudy, B. (1986) Interactions between membranes and cytolytic peptides. *Biochim. Biophys. Acta 864*, 123−141.
(8) Clements, J. A. (1957) Surface tension of lung extracts. *Proc. Soc. Exp. Biol. Med. 95*, 170−172.
(9) Pattle, R. E. (1958) Properties, function, and origin of the alveolar lining layer. *Proc. R. Soc. London, Ser. B 148*, 217−240.
(10) Sansom, M. S. (1991) The biophysics of peptide models of ion channels. *Prog. Biophys. Mol. Biol. 55*, 139−235.
(11) Landgraf, B., Cohen, F. E., Smith, K. A., Gadski, R., and Ciardelli, T. L. (1989) Structural significance of the C-terminal amphiphilic helix of interleukin-2. *J. Biol. Chem. 264*, 816−822.

(12) DeVries, A. L. (1984) Role of glycopeptides and peptides in inhibition of crystallization of water in polar fishes. *Philos. Trans. R. Soc., B 304*, 575−588.
(13) Duman, J. G. (1982) Insect antifreezes and ice-nucleating agents. *Cryobiology 19*, 613−627.
(14) Crisma, M., Formaggio, F., Moretto, A., and Toniolo, C. (2006) Peptide helices based on α-amino acids. *Biopolymers 84*, 3−12.
(15) Marechal, Y. (2007) *The Hydrogen Bond and the Water Molecule: The Physics and Chemistry of Water, Aqueous and Bio-Media*, Elsevier, Amsterdam.
(16) Vieira-Pires, R. S., and Morais-Cabral, J. H. (2010) 3_{10}-helices in channels and other membrane proteins. *J. Gen. Physiol. 136*, 585−592.
(17) Jr, R. B., and Eliezer, D. (2003) A structural and functional role for 11-mer repeats in α-synuclein and other exchangeable lipid binding proteins. *J. Mol. Biol. 329*, 763−778.
(18) Segrest, J. P., Jones, M. K., Klon, A. E., Sheldahl, C. J., Hellinger, M., Loof, H. D., and Harvey, S. C. (1999) A detailed molecular belt model for apolipoprotein A-I in discoidal high density lipoprotein. *J. Biol. Chem. 274*, 31755−31758.
(19) Sheinerman, F. B., and Brooks, C. L. (1995) 3_{10}-helices in peptides and proteins as studied by modified Zimm-Bragg theory. *J. Am. Chem. Soc. 117*, 10098−10103.
(20) Barlow, D. J., and Thornton, J. M. (1988) Helix geometry in proteins. *J. Mol. Biol. 201*, 601−619.
(21) Topol, I. A., Burt, S. K., Deretey, E., Tang, T. H., Perczel, A., Rashin, A., and Csizmadia, I. G. (2001) α- and 3_{10}-helix interconversion: A quantum-chemical study on polyalanine systems in the gas phase and in aqueous solvent. *J. Am. Chem. Soc. 123*, 6054−6060.
(22) Smythe, M. L., Huston, S. E., and Marshall, G. R. (1995) The molten helix: Effects of solvation on the α-helical to 3_{10}-helical transition. *J. Am. Chem. Soc. 117*, 5445−5452.
(23) Gerstein, M., and Chothia, C. H. (1991) Analysis of protein loop closure: Two types of hinges produce one motion in lactate dehydrogenase. *J. Mol. Biol. 220*, 133−149.
(24) McPhalen, C. A., Vincent, M. G., Picot, P., and Jansonius, J. N. (1992) Domain closure in mitochondrial aspartate aminotransferase. *J. Mol. Biol. 227*, 197−213.
(25) Karle, I. L., and Balaram, P. (1990) Structural characteristics of α-helical peptide molecules containing Aib residues. *Biochemistry 29*, 6747−6756.
(26) Otoda, K., Kitagawa, Y., Kimura, S., and Imanishi, Y. (1993) Chain length dependent transition of 3_{10}- to α-helix of Boc-$(Ala\text{-}Aib)_n$-OMe. *Biopolymers 33*, 1337−1345.
(27) Karle, I. L., Sukumar, M., and Balaram, P. (1986) Parallel packing of α-helices in crystals of the zervamicin IIA analog Boc-Trp-Ile-Ala-Aib-Ile-Val-Aib-Leu-Aib-Pro-OMe·$2H_2O$. *Proc. Natl. Acad. Sci. U.S.A. 83*, 9284−9288.
(28) Karle, I. L., Flippen-Anderson, J. L., Sukumar, M., and Balaram, P. (1988) Monoclinic polymorph of Boc-Trp-Ile-Ala-Aib-Ile-Val-Aib-Leu-Aib-Pro-OMe(anhydrous). Parallel packing of 3_{10}-/α-helices and a transition of helix type. *Int. J. Pept. Protein Res. 31*, 567−576.
(29) Marshall, G. R., Hodgkin, E. E., Langs, D. A., Smith, G. D., Zabrocki, J., and Leplawy, M. T. (1990) Factors governing helical preference of peptides containing multiple α,α-dialkyl amino acids. *Proc. Natl. Acad. Sci. U.S.A. 87*, 487−491.
(30) Aleman, C., Subirana, J. A., and Perez, J. J. (1992) A molecular mechanical study of the structure of poly(α-aminoisobutyric acid). *Biopolymers 32*, 621−631.
(31) Hodgkin, E. E., Clark, J. D., Miller, K. R., and Marshall, G. R. (1990) Conformational analysis and helical preferences of normal and α,α-dialkyl amino acids. *Biopolymers 30*, 533−546.
(32) Huston, S. E., and Marshall, G. R. (1994) α/3_{10}-helix transitions in α-methylalanine homopeptides: Conformational transition pathway and potential of mean force. *Biopolymers 34*, 75−90.
(33) Bellanda, M., Mammi, S., Geremia, S., Demitri, N., Randaccio, L., Broxterman, Q. B., Kaptein, B., Pengo, P., Pasquato, L., and Scrimin, P. (2007) Solvent polarity controls the helical conformation of short peptides rich in C^{α}-tetrasubstituted amino acids. *Chem.—Eur. J. 13*, 407−416.
(34) Karle, I. L., Flippen-Anderson, J. L., Gurunath, R., and Balaram, P. (1994) Facile transition between 3_{10}- and α-helix: Structures of 8-, 9-, and 10-residue peptides containing the -$(Leu\text{-}Aib\text{-}Ala)_2$-Phe-Aib-fragment. *Protein Sci. 3*, 1547−1555.
(35) Vijayakumar, E. K., and Balaram, P. (1983) Stereochemistry of α-aminoisobutyric acid peptides in solution: Helical conformations of protected decapeptides with repeating Aib-L-Ala and Aib-L-Val sequences. *Biopolymers 22*, 2133−2140.
(36) Nardini, M., Lang, D. A., Liebeton, K., Jaeger, K., and Dijkstra, B. W. (2000) Crystal structure of *Pseudomonas aeruginosa* lipase in the open conformation. *J. Biol. Chem. 275*, 31219−31225.
(37) Borhani, D. W., Rogers, D. P., Engler, J. A., and Brouillette, C. G. (1997) Crystal structure of truncated human apolipoprotein A-I suggests a lipid-bound conformation. *Proc. Natl. Acad. Sci. U.S.A. 94*, 12291−12296.
(38) Cornell, W. D., Cieplak, P., Bayly, C. I., Gould, I. R., Merz, K. M. J., Ferguson, D. M., Spellmeyer, D. C., Fox, T., Caldwell, J. W., and Kollman, P. A. (1995) A second generation force field for the simulation of proteins, nucleic acids, and organic molecules. *J. Am. Chem. Soc. 117*, 5179−5197.
(39) Jorgensen, W. L., Chandrasekhar, J., Madura, J. D., Impey, R. W., and Klein, M. L. (1983) Comparison of simple potential functions for simulating liquid water. *J. Chem. Phys. 79*, 926−935.
(40) Case, D. A., Darden, T. A., Cheatham, T. E. I., Simmerling, C. L., Wang, J., Duke, R. E., Luo, R., Crowly, M., Walker, R. C., Zhang, W., Merz, K. M., Wang, B., Hayik, S., Roitberg, A., Seabra, G., Kolossvry, I., Wong, K. F., Pasani, F., Vanicek, J., Wu, X., Brozell, S. R., Steinbrecher, T., Gohlke, H., Yang, L., Tan, C., Mongan, J., Hornak, V., Cui, G., Mathews, D. H., Seetin, M. G., Sagui, C., Babin, V., and Kollman, P. A. (2008) Amber molecular dymnamics package. *AMBER 10*, University of California, San Francisco.
(41) Johnson, Q. R., Nellas, R. B., and Shen, T. (2012) Solvent-dependent gating motions of an extremophilic lipase from *Pseudomonas aeruginosa*. *Biochemistry 51*, 6238−6245.
(42) Kabsch, W., and Sander, C. (1983) Dictionary of protein secondary structure: Pattern recognition of hydrogen-bonded and geometrical features. *Biopolymers 22*, 2577−2637.
(43) Armen, R., Alonso, D. O. V., and Daggett, V. (2003) The role of α-, 3_{10}-, and π-helix in helix to coil transitions. *Protein Sci. 12*, 1145−1157.
(44) Mikhonin, A., Bykov, S., Myshakina, N., and Asher, S. (2006) Peptide secondary structure folding reaction coordinate: Correlation between UV Raman amide III frequency, Ψ Ramachandran angle, and hydrogen bonding. *J. Phys. Chem. B 110*, 1928−1943.
(45) Nellas, R. B., Glover, M. M., Hamelberg, D., and Shen, T. (2012) High-pressure effect on the dynamics of solvated peptides. *J. Chem. Phys. 136*, 145103.
(46) Johnson, Q., Doshi, U., Shen, T., and Hamelberg, D. (2010) Water's contribution to the energetic roughness from peptide dynamics. *J. Chem. Theory Comput. 6*, 2591−2597.
(47) Ogino, H., Katou, Y., Akagi, R., Mimitsuka, T., Hiroshima, S., Gemba, Y., Doukyu, N., Yasuda, M., Ishimi, K., and Ishikawa, H. (2007) Cloning and expression of gene, and activation of an organic solvent-stable lipase from *Pseudomonas aeruginosa* LST-03. *Extremophiles 11*, 809−817.
(48) Ogino, H., Nakagawa, S., Shinya, K., Muto, T., Fujimura, N., Yasuda, M., and Ishikawa, H. (2000) Purification and characterization of organic solvent-stable lipase from organic solvent-tolerant *Pseudomonas aeruginosa* LST-03. *J. Biosci. Bioeng. 89*, 451−457.
(49) Henchman, R. H., and McCammon, J. A. (2002) Extracting hydration sites around proteins from explicit water simulations. *J. Comput. Chem. 23*, 861−869.
(50) Ogino, H. (2008) in *Protein adaptation in extremophiles* (Siddiqui, K. S., and Thomas, T., Eds.) pp 193−236, Nova Biomedical, New York.
(51) Uttatree, S., Winayanuwattikun, P., and Charoenpanich, J. (2010) Isolation and characterization of a novel thermophilic-organic

solvent stable lipase from *Acinetobacter baylyi*. *Appl. Biochem. Biotechnol. 162*, 1362−1376.
(52) Haynes, W. H. (2013) *CRC Handbook of Chemistry and Physics*, 94th ed., CRC Press, Inc., Boca Raton, FL.
(53) Reichardt, C. (2003) *Solvents and Solvent Effects in Organic Chemistry*, 3rd ed., Wiley, Weinheim, Germany.